Novel glycosylated mycosporine-like amino acids with radical scavenging activity from the cyanobacterium Nostoc commune

Novel glycosylated mycosporine-like amino acids with radical scavenging activity from the cyanobacterium *Nostoc commune*

Kei Matsui[1], Ehsan Nazifi[3], Shinpei Kunita[1], Naoki Wada[2], Seiichi Matsugo[2] and Toshio Sakamoto[1, 2, 3,*]

[1]Division of Biological Sciences, Graduate School of Natural Science and Technology, Kanazawa University. Kakuma, Kanazawa 920-1192, Japan.

[2]School of Natural System, College of Science and Engineering, Kanazawa University. Kakuma, Kanazawa 920-1192, Japan.

[3]Division of Life Science, Graduate School of Natural Science and Technology, Kanazawa University. Kakuma, Kanazawa 920-1192, Japan.

*__Address for correspondence:__

Dr. Toshio Sakamoto

School of Natural System, College of Science and Engineering, Kanazawa University. Kakuma, Kanazawa 920-1192, Japan.

Phone: +81-76-264-6227

Fax: +81-76-264-6215

E-mail: tsakamot@staff.kanazawa-u.ac.jp

Abstract

Mycosporine-like amino acids (MAAs) are UV absorbing pigments, and structurally distinct MAAs have been identified in taxonomically diverse organisms. Two novel MAAs were purified from the cyanobacterium *Nostoc commune*, and their chemical structures were characterized. An MAA with an absorption maximum at 335 nm was identified as a pentose-bound porphyra-334 derivative with a molecular mass of 478 Da. Another identified MAA had double absorption maxima at 312 and 340 nm and a molecular mass of 1050 Da. Its unique structure consisted of two distinct chromophores of 3-aminocyclohexen-1-one and 1,3-diaminocyclohexen and two pentose and hexose sugars. These MAAs had radical scavenging activity *in vitro*; the 1050-Da MAA contributed approximately 27% of the total radical scavenging activities in a water extract of *N. commune*. These results suggest that these glycosylated MAAs have multiple roles as a UV protectant and an antioxidant relevant to anhydrobiosis in *N. commune*.

High lights

> Two novel glycosylated MAAs were found in *Nostoc commune*. > The 478-Da MAA was identified as a pentose-bound porphyra-334 derivative. > The 1050-Da MAA consisted of two distinct chromophores, pentose and hexose. > These MAAs had radical scavenging activity.

Key words: anhydrobiosis; antioxidant; glycosylation; porphyra-334; UV protectant

1. Introduction

Certain desiccated organisms have no metabolic activity and are able to rapidly resume metabolism upon rehydration in a phenomenon termed “anhydrobiosis” [1-5]. The cyanobacterium *Nostoc commune* can retain viability for over 100 years following desiccation [6, 7]. Thus, *N. commune* is considered an anhydrobiotic microorganism with oxygenic photosynthetic capabilities without differentiation into akinetes (spores) [8-10]. The mechanism of extreme desiccation tolerance by this species is thought to involve multiple processes that include extracellular polysaccharide (EPS) production, compatible solute accumulation, regulation of photosynthesis and protection from UV radiation.

In natural habitats, *N. commune* forms visible colonies in which cellular filaments embed within biochemically complex extracellular matrices [11]. EPS are major components of the extracellular matrices and account for 80% of the dry weight of *N. commune* colonies [12]. The production of EPS is widely known in cyanobacteria [13, 14], and it is thought that EPS play a major role in cyanobacteria in protecting cells from various stresses in severe habitats [15-17]. Removal of EPS in *N. commune* causes a significant reduction in the stress tolerance of photosynthesis during desiccation and freeze-thawing [18].

Anhydrobiotic organisms accumulate trehalose (α-D-glucopyranosyl-[1, 1]-α-D-glucopyranoside) as a compatible solute. Trehalose protects biological membranes and proteins against the deleterious effects of water removal by replacing hydrating water molecules and forming amorphous glasses (vitrification) [2-4]. In *N. commune*, trehalose accumulation occurs in response to water loss during desiccation [19], and specific inhibition of trehalase controls trehalose accumulation [20]. The trehalose accumulation capacity of *N. commune* is similar to that of the drought-resistant cyanobacteria *Phormidium autumnale* and *Chroococcidiopsis* sp. [19, 21]. Therefore, trehalose accumulation is thought to be relevant to cyanobacterial desiccation tolerance.

N. commune colonies are naturally subjected to regular cycles of desiccation and wetting. Photosynthetic activity recovers rapidly following rehydration [18, 19, 22, 23]. As the water content decreases during desiccation, photosynthetic activity decreases, and no photosynthetic activity is detected in desiccated colonies [19]. This cessation of photosynthetic electron transport during desiccation is thought to be a protective response to avoid light-induced damage by suppressing reactive oxygen species production [24, 25]; however, the mechanisms regulating photosynthesis remain unknown.

Mycosporine-like amino acids (MAAs) are water-soluble pigments that absorb UV radiation of 280 to 340 nm, and structurally distinct MAAs are known in taxonomically diverse organisms [26-31]. Recently, Balskus and Walsh [32] have shown that sedoheptulose 7-phosphase, which is a pentose phosphate pathway intermediate, is a precursor to 4-deoxygadusol in MAA biosynthesis, and they have also identified the genes responsible in the sequential conversion of 4-deoxygadusol to mycosporine-glycine and shinorine. In cyanobacteria, MAAs function mainly to protect the cells against solar radiation [33, 34]. Because the energy absorbed by MAAs is promptly dispersed into the surroundings as heat [35, 36], MAAs do not function as accessory pigments in photosynthesis [28]. In *N. commune*, a structurally unique MAA covalently bound to oligosaccharides has been reported [37], and the glycosylated structure of this MAA is thought to allow for the interaction with extracellular matrices [11]. The hydrophobic pigment scytonemin absorbs UV-A radiation of 320 to 400 nm [38] and occurs exclusively in the cyanobacterial sheath [39]. With both the UV-absorbing pigments of MAAs and scytonemin in its extracellular matrices [11], *N. commune* is thought to be able to adapt to terrestrial environments with high levels of solar radiation.

Desiccated *N. commune* has extreme longevity [7], implying the involvement of antioxidants protecting biomolecules from oxidation. Fe-superoxide dismutase (SodF) is the

third most abundant water-soluble protein in *N. commune* [40]. Thus, we characterized low-molecular-weight antioxidants in *N. commune*. In our study, the radical scavenging activity related to MAA was found in water extracts from desiccated colonies of *N. commune*. Here, we report the characterization of two novel and unique MAAs from *N. commune* with radical scavenging ability. These findings provide new insights into the diversity of MAAs as well as their biological functions in adaptation to terrestrial environments.

2. Materials and Methods

2.1. Microorganisms

Colonies of *Nostoc commune* growing in the field were collected from the Kakuma Campus of Kanazawa University (N 36.547187, E 136.70537) or Tsubata Shinrin Kohen, Ishikawa, Japan (N 36.689282, E 136.749058) from April to November. Wet colonies naturally swelled after rain in the field were harvested, washed with tap water to remove soil, air-dried in the laboratory, and stored at room temperature until used. The MAA was extracted with water from *N. commune* powder and the UV-VIS absorption spectrum was measured. The MAA concentration was estimated spectrophotometrically with an extinction coefficient of 120 liters g^{-1} cm^{-1} [33]. Two types of *N. commune* characterized by differences in their absorption spectra of water extracts were found, and each *N. commune* sample was separately used for MAA purification.

2.2. Purification of an MAA with an absorption maximum at 335 nm

Dry colonies of *N. commune* (32 g) containing an MAA with an absorption maximum at 335 nm were frozen with liquid nitrogen and ground with a mortar and pestle. The *N. commune* powder was suspended in 30% methanol (1.5 L) and left at 4˚C overnight. The extract was filtrated with double coarse paper filters (Kimwipe, CRECIA), and the filtrate was

centrifuged at 4,200 x *g* for 20 min at 4˚C. The supernatant was vacuum-filtered with a Buchner funnel type sintered-glass filter. The filtrate was concentrated with a rotary evaporator under reduced pressure, and the solvent was changed to 400 ml of 100% methanol. The methanol insoluble fraction was removed by centrifugation at 7,000 x g for 10 min at 4˚C, and the supernatant was vacuum-concentrated to change the solvent to 150 ml of 30% methanol. After removal of 30% methanol insoluble materials by centrifugation at 7,000 x g for 10 min at 4˚C, the supernatant was vacuum-concentrated again to change the solvent to 50 ml of 100% methanol. After centrifugation at 7,000 x g for 10 min at 4˚C, the supernatant was vacuum-concentrated to change the solvent to 8.5 ml of 0.2% acetic acid. After centrifugation at 21,500 x g for 10 min for 4˚C, the supernatant was injected into an HPLC system equipped with a reverse phase column (IRICA C18, 20 x 250 mm). The mobile phase was 0.2% acetic acid at a flow rate of 3 ml min^{-1}. A_{330} was monitored with a Hitach L-4200 UV-VIS detector. The fraction containing the MAA was recovered, condensed with a rotary evaporator and injected to a liquid chromatography system (Biologic LP, Bio rad) with a gel filtration column (Toyopearl HW50, 20 x 200 mm). The mobile phase was water at a flow rate of 1 ml min^{-1}, and A_{280} was monitored with a Bio-rad UV detector. The MAA fraction was recovered and condensed with a rotary evaporator, and the final MAA product was lyophilized. To determine the extinction coefficient of the purified MAA with an absorption maximum at 335 nm, 1 ml of the solution in water (approximately 5 mg ml^{-1}) was prepared, and its A_{335} was determined. The dry weight of the MAA in the 1 ml solution was measured after lyophilization.

2.3. Purification of an MAA with absorption maxima at 312 and 340 nm

N. commune powder (5 g) containing an MAA with absorption maxima at 312 and 340 nm was suspended in distilled water (200 ml), and the MAA was extracted with stirring at 4˚C for

1 h in the dark. After centrifugation at 8,270 x g for 20 min at 4˚C, the supernatant was vacuum-filtered with a Buchner funnel type sintered-glass filter. Ethanol was added to the filtrate to result in a final concentration of 70%, and the mixture was left at 4˚C for 1 h in the dark to precipitate 70% ethanol-insoluble materials. After centrifugation at 8,270 x g for 20 min at 4˚C, the supernatant was vacuum-filtered with a Buchner funnel type sintered-glass filter. The filtrate was concentrated with a rotary evaporator under reduced pressure and centrifuged at 21,500 x g for 10 min at 4˚C. The supernatant was filtrated though a 0.20-μm syringe filter (Minisart RC 15, Sartorius Stedim) and injected into a HPLC system equipped with a reverse phase column (IRICA C18, 20 x 250 mm). The MAA was adsorbed with 0.2% acetic acid as a mobile phase and eluted with 0.1% acetic acid 10% methanol. The flow rate was constant at 3 ml min^{-1}, and the A_{330} was monitored with a Hitach L-4200 UV-VIS detector. The fraction containing the MAA was recovered, condensed with a lyophilizer and injected into a liquid chromatography system (Biologic LP, Bio rad) with a gel filtration column (Toyopearl HW50, 20 x 200 mm). The mobile phase was water at a flow rate of 1 ml min^{-1}, and A_{280} was monitored with a Bio-rad UV detector. The MAA fraction was recovered, and the final product of the MAA was lyophilized. To determine the extinction coefficient of the purified MAA with absorption maxima at 312 and 340 nm, 1 ml of the solution in water (approximately 3.6 mg ml^{-1}) was prepared, and its A_{312} was determined. The dry weight of the MAA in the 1 ml solution was measured after lyophilization.

2.4. Thermal decomposition of the MAA with absorption maxima at 312 and 340 nm

The purified MAA with absorption maxima at 312 and 340 nm was treated at 100˚C for 6 h in a solution of 0.1% acetic acid and 10% methanol. The decomposition was monitored by changes of absorption spectrum. The thermal decomposed products were analyzed at the Center for Development of Biotech Industries, Kazusa DNA Institute, with a LC-Orbitrap

mass spectrometer composed of a liquid chromatograph (Aginent 1200 series) and a linear ion trap mass spectrometer (Finnigan LTQ ORBITRAP XL). The absorption spectra were recorded with a photodiode array detector.

2.5. MALDI-TOF MS analysis

MALDI-TOF MS analysis was performed at the Division of Functional Genomics, Advanced Science Research Center, Kanazawa University, with a tandem mass spectrometer (4800 plus MALDI TOF/TOF™ Analyzer; Applied Biosystems, Foster City, CA) using 2,5-dihydroxybenzoic acid (DHB) as a matrix. The secondary mass spectrum was recorded when applicable.

2.6. LC-MS/MS analysis

Liquid chromatography tandem mass spectrometry (LC-MS/MS) analysis was performed at the Center for Development of Biotech Industries, Kazusa DNA Institute, with a LC-Orbitrap MS composed of a liquid chromatograph (Aginent 1200 series) and a linear ion trap mass spectrometer (Finnigan LTQ ORBITRAP XL).

2.7. Spectroscopic methods

UV-VIS spectra were recorded with a Hitachi U-2800 spectrophotometer. Fourier transformation infrared (FTIR) spectra were recorded with a Jasco FT/IR-230 FTIR spectrometer using the KBr disk method. NMR spectra in D_2O solvent were recorded with a Bruker Avance 750 at the Suntory Institute for Bioorganic Research or with a JOEL ECA600 spectrometer at the Research Institute for Instrumental Analysis in Kanazawa University. Either 4,4-dimethyl-4-silapentane-1-sulfonic acid (DSS) or 3-(trimethylsilyl)propanoic acid (TMP) was used as an internal NMR standard.

2.8. Measurement of Trolox equivalent antioxidant capacity (TEAC)

Radical scavenging activity was measured using 2,2'-azino-bis (3-ethylbenzothiazoline-6-sulfonic acid) (ABTS) as a substrate in a colorimetry assay [41]. Decolorization of the A_{734} was monitored photospectrometrically for 1 h. Electron spin resonance (ESR) signals of ABTS or 2,2-diphenyl-1-picrylhydrazyl (DPPH) were recorded using a free radical monitor (JOEL JES-FR30EX). Trolox (6-hydroxy-2,5,7,8-tetramethylchroman-2-carboxylic acid) was used as a standard.

2.9. Chromatographic separation and detection of the MAA and radical scavenging activity in water extract of N. commune

N. commune powder (100 to 200 mg) was suspended in distilled water (20 to 40 ml) and extracted at room temperature with stirring for 1 h. After centrifugation at 21,500 x g for 10 min at 4˚C, the supernatant was concentrated with a centrifugal concentrator (VC-360, TAITEC) and filtered through a 0.20-μm syringe filter (Minisart RC 15, Sartorius Stedim). The concentrated water extract containing 170 nmol TEAC was injected into an HPLC system with a Hitachi L-6200 pump and an L-4200 UV-VIS detector equipped with a reverse phase column (Wakosil 5C18, 4.6 mm × 250 mm; Wako, Osaka, Japan). For analysis of water extract with the 1050-Da MAA, the mobile phase changed stepwise from 0.2% acetic acid for the initial 16 min, 0.1% acetic acid 5% methanol for the next 52 min and 100% methanol for the final 42 min. For anlysis of water extract with the 478-Da MAA, the mobile phase was 0.2% acetic acid for the initial 30 min and 100% methanol for the next 36 min. The flow rate was constant at 0.5 ml min^{-1} and a 1 ml fraction was collected every 2 min. The MAA was detected by A_{330}. Radical scavenging activity was measured by the ABTS decolorization assay.

3. Results

3.1. Two types of MAA in N. commune

During the characterization of MAA in field isolated natural colonies of *N. commune*, two types of *N. commune* colonies whose water extracts resulted in different UV-absorbing spectra were found, although no obvious differences in their appearance could be observed by eye. One MAA isolate showed a single absorption maximum at 335 nm, and the other MAA isolate showed an absorption maximum at 312 nm associated with a shoulder at 340 nm. These MAAs had different retention times when analyzed by HPLC, indicating different chemical structures. Each MAA was found separately, but biological or physiological differences allowing us to separate these *N. commune* samples could not be specified. Thus each *N. commune* sample was used for MAA purification and characterization separately.

3.2. MAA with an absorption maximum at 335 nm

An MAA with an absorption maximum at 335 nm was purified from field isolated natural colonies of *N. commune* (Table 1). The UV absorption spectrum of the purified MAA showed a single absorption peak at 335 nm (Fig. 1A), and the absorption coefficient of this MAA was 69.4 L g^{-1} cm^{-1} at 335 nm in water. The molecular mass was 478 Da as determined by MALDI-TOF MS analysis (Fig S1A). The calculated molar absorption coefficient at 335 nm was 33173 M^{-1} cm^{-1}. Because no MAA with a molecular mass of 478 Da has been reported, the chemical structure of the 478 Da MAA was further characterized.

The IR spectrum of the 478 Da MAA (Fig. S2A) was compared with those of the known MAAs palythine [42] and porphyra-334 [43] (Table 3). Similar IR absorption peaks were observed, suggesting that the 478-Da MAA has similar structure to these MAAs. The characteristic absorption peak at 3400 cm^{-1} but not 3300 cm^{-1} in the 478-Da MAA suggests a large number of hydroxyl groups present in this molecule, consistent with the presence of a

pentose ring as described below.

MALDI-TOF MS/MS analysis was performed on the molecular ion fragment with m/z 479 (Fig. S3). A fragment with m/z 347 was detected in the second MS, and this molecular mass was identical to that of porphyra-334 [44]. The neutral loss of 132 suggests the deletion of a pentose ($C_5H_8O_4$) from the parent molecular ion with m/z 479. The fragments with m/z 435 and m/z 420 suggest the deletion of CO_2 and CH_3, and this fragmentation pattern was similar to the results of the MS analysis of the known MAA [45]. These data suggest that the 478-Da MAA is a porphyra-334 derivative bound with pentose. This was confirmed by NMR analysis (Table 3). Both known chemical shifts for porphyra-334 and pentose were observed in the 478-Da MAA. According to the heteronuclear multiple band correlation (HMBC) spectrum, a correlation between the C7 carbon in the porphyra-334 structure and the proton bound at the C1 carbon of pentose was observed, suggesting that pentose is bound to the C7 position of porphyra-334 via an *O*-glycoside bond. Figure 2 shows the predicted structure for the 478-Da MAA from *N. commune*.

3.4. An MAA with absorption maxima at 312 and 340 nm

An MAA with absorption maxima at 312 and 340 nm was purified from field isolated natural colonies of *N. commune* (Table 2). The purified MAA showed a characteristic UV absorption spectrum with an absorption peak at 312 nm associated with a shoulder at 340 nm (Fig. 1B), and its absorption coefficient was 56.0 L g^{-1} cm^{-1} at 312 nm in water. This UV absorption spectrum suggests the presence of two distinct chromophores, 3-aminocyclohexen-1-one and 1,3-diaminocyclohexen, related to the absorption peaks at 312 nm and 340 nm, respectively. The molecular mass was 1050 Da as determined by MALDI-TOF MS analysis (Fig. S1B), indicating a novel MAA with a unique chemical structure. The calculated molar absorption

coefficient at 312 nm was 58800 M^{-1} cm^{-1}. The characteristic absorption peak at 3399 cm^{-1} in the IR spectrum of the 1050-Da MAA (Fig. S2B) suggests that a large number of hydroxyl groups present in this molecule, consistent with the presence of pentose and hexose in this molecule as described below.

Multiple MS analysis was performed on the molecular ion fragment with m/z 1051 (Table S1). A fragment with m/z 1015 was detected in the MS^2 representing the deletion of 2 molecules of H_2O. In the MS^3, a fragment with m/z 883 was detected, suggesting the deletion of pentose ($C_5H_8O_4$ with a mass of 132). A fragment with m/z 721 in the MS^4 suggests the deletion of hexose ($C_6H_{10}O_5$ with a mass of 162). A fragment with m/z 649 detected in the MS^3 and MS^4 was considered a core MAA produced by the deletion of pentose and hexose. Finally, the fragment with m/z 649 showed a characteristic mass spectrum similar to known MAAs in the MS^5.

To characterize the structure of the 1050-Da MAA further, thermal decomposition products were analyzed with LC-MS (Fig. S4, Table S2). In the thermal decomposition products, a fragment with a single absorption peak at 312 nm related to a 3-aminocyclohexen-1-one derivative and a fragment with a single absorption peak at 335 nm related to a 1,3-diaminocyclohexen derivative were detected separately (Fig. S4). The predicted formula of the 1050-Da MAA was $C_{45}H_{70}N_4O_{24}$, consisting of 2 molecules of H_2O, pentose, hexose, a $C_{13}H_{22}N_2O_6$ unit and a $C_{21}H_{26}N_2O_7$ unit; the fragments related to the removal of those units were detected in the thermal decomposition products (Table S2A) and also in the mass spectra of the 1050-Da MAA (Table S1). The fragments related to the deletion of a $C_8H_{10}O_4$ unit of 170 Da were detected (Table S2B); this 170-Da unit could be related to 4-deoxygadusal, which is a precursor for the biosynthesis of MAA and includes a core ring [32]. These results support the presence of multiple chromophores in the 1050-Da MAA. The 1050-Da MAA also degraded to pentose, hexose, a $C_{14}H_{23}N_1O_8$ unit and a

$C_{20}H_{29}N_3O_7$ unit during the thermal decomposition (Table S2C). These data also suggest that the 1050-Da MAA contains two distinct chromophores of 3-aminocyclohexen-1-one and 1,3-diaminocyclohexen, pentose and hexose (Fig. 3A-D).

^{13}C and ^{1}H NMR spectra of the 1050-Da MAA were recorded and compared with those of porphyra-334 and mycosporine-glycine (Table 5). In the ^{13}C-NMR spectrum, signals with identical chemical shifts to both porphyra-334 and mycosporine-glycine were observed, suggesting the presence of two distinct chromophores, 3-aminocyclohexen-1-one and 1,3-diaminocyclohexen. In the ^{1}H-NMR spectrum, the signals related to the 3-aminocyclohexen-1-one ring accounted for 4 protons equivalent per molecule (Table 5), suggesting the 1050-Da MAA contains a single 3-aminocyclohexen-1-one with an absorption maximum at 335 nm. The signals related to the 1,3-diaminocyclohexen ring accounted for 8 protons equivalent per molecule (Table 5), suggesting the 1050-Da MAA contains two 1,3-diaminocyclohexen molecules with an absorption maximum at 312 nm. These results are consistent with the absorption spectrum (Fig. 1A) and MS analysis of the 1050-Da MAA. Two separable signals characteristic of the C1 positions of distinct sugars were observed, confirming the presence of two sugars (Table 5), although their molecular species and coupling scheme were unidentified. In the ^{13}C NMR spectrum, two signals related to a carboxyl group were observed, suggesting the presence of two carboxyl groups per molecule. After combining the data from the MS and NMR analysis, a predicted structure of the 1050-Da MAA is shown in Figure 3E.

3.5. Radical scavenging activity in MAAs

Table 6 shows the radical scavenging activity detected in the purified MAAs from *N. commune*. Both the 478-Da MAA and the 1050-Da MAA showed ABTS radical scavenging activity when we monitored the decolorization of ABTS radicals. During the time course

experiments, decolorization of ABTS radicals increased as incubation times increased from 10 min to 3 h, suggesting that these MAAs are slow-acting radical scavengers. The molecule used as a standard, Trolox, is known to be a fast-acting scavenger in which the reaction completes within 10 min. Based on these results, the incubation time was fixed for 1 h in the assay. When we directly monitored the decrease of ABTS radicals by ESR, the activity of the 478-Da MAA was equivalent to that of Trolox, and the 1050-Da MAA showed higher activity than did Trolox (Table 6). The DPPH radical is known to have selectivity for scavengers with a strong radical scavenging activity [46]. When DPPH was used as a substrate, the 1050-Da MAA was capable of scavenging DPPH radicals, but no activity was detected in the 478-Da MAA (Table 6). These results indicate that the 1050-Da MAA is a strong radical scavenger that reacts with both ABTS and DPPH organic radicals *in vitro*.

The radical scavenging activity related to the 1050-Da MAA was examined in the water extract of *N. commune* by HPLC analysis (Fig. 4). The elution peak of the 1050-Da MAA was identified by comparing with the purified 1050-Da MAA and with the characteristic absorption spectrum with absorption maxima at 312 nm and 340 nm. At least three other MAAs or MAA derivatives were detected, but the 1050-Da MAA accounted for approximately 47% of total MAAs (Fig. 4A). The radical scavenging activity eluted together with the 1050-Da MAA in the same fractions and the 1050-Da MAA associated activity accounted for approximately 27% of the total recovered activity (Fig. 4B). These results suggest that the 1050-Da MAA is a major MAA in *N. commune* colonies with this type of MAA and also a main component of the water-soluble radical scavengers.

The water extract of *N. commune* with the 478-Da MAA was examined by HPLC analysis (Fig. 5). The 478-Da MAA was a main MAA detected in the water-soluble extract of *N. commune* with this type of MAA (Fig. 5A). Interestingly, high radical scavenging activity not associated with the 478-Da MAA was detected (Fig. 5B). This suggests that extra

water-soluble antioxidants contribute to the total level of radical scavenging capacity in *N. commune* colonies with the 478-Da MAA, which showed lower activity than the 1050-Da MAA (Table 6). There are two types of *N. commune* in terms of water-soluble antioxidants consistent with the types of MAAs. Characterization of water-soluble antioxidants in *N. commune* colonies with the 478-Da MAA is currently under way.

4. Discussion

Novel glycosylated MAAs with radical scavenging activities were found in the cyanobacterium *Nostoc commune* examined in this study. Two types of *N. commune* characterized by the different MAAs found, although biological and physiological conditions allowing the separation of these types are unknown. Both a 478-Da MAA (Fig. 2) and a 1050-Da MAA (Fig. 3) were bound with sugars, and their chemical structures were different from the previously reported MAA in *N. commune* [37]. The novel 1050-Da MAA consisted of three chromophores, including both 3-aminocyclohexen-1-one and 1,3-diaminocyclohexen (Fig. 3), and this structural feature was related to the expanded UV-absorbing window due to its unique double absorption maxima covering both UV-A and UV-B wavelengths (Fig. 1B). This is the first report of an MAA with both 3-aminocyclohexen-1-one and 1,3-diaminocyclohexen within a single molecule. The *in vitro* experiments demonstrated a potent radical scavenging activity in these novel *N. commune* MAAs (Table 6, Fig. 4). These results suggest that these unique glycosylated MAAs function as UV protectants and antioxidants relevant to anhydrobiosis in *N. commune*. Without these glycosylated MAAs *N. commune* maybe incapable of surviving terrestrial environments and of sustaining viability in a desiccated state; however, physiological roles of these MAAs in this unique organism remain to be elucidated in future studies.

Previously identified MAAs have a low molecular weight of approximately 400 Da

and are composed of either a 3-aminocyclohexen-1-one or a 1,3-diaminocyclohexen chromophore with single absorption peak at around 310 nm or 330 nm [28, 29, 31]. In this study, we identified a *N. commune* 1050-Da MAA with both 3-aminocyclohexen-1-one and 1,3-diaminocyclohexen chromophores (Fig. 3). In addition to broadening the UV absorption profile (Fig. 1B), the conjugation of 3-aminocyclohexen-1-one rings is thought to lead to an antioxidant role for the 1050-Da MAA (Table 6, Fig. 4). Because cyanobacterial unidentified MAAs with the double absorption maxima, including one from *N. commune*, have been reported [33, 37, 47-49], this type of combined MAAs may be distributed throughout cyanobacteria. The finding of the 1050-Da MAA from *N. commune* provides new insight into the molecular diversity of MAAs as well as mechanisms to adapt to terrestrial environments; however, the biosynthesis of the 1050-Da MAA in *N. commune* and the mechanisms of action for UV absorption and radical scavenging abilities in a single molecule remain to be elucidated in future studies.

Consistent with our results, a xylose-containing UV-absorbing compound has been suggested to be present in *N. commune* [48], and an interaction via its sugar moiety with the WspA protein, a major protein in the extracellular matrices [12, 50], contributes to the construction of extracellular matrices [11, 48]. It is noteworthy that all three of the MAAs identified thus far in *N. commune* are glycosylated (Fig. 2, 3)[37]. Known glycosylated MAAs mycosporine-glutaminol-glucoside and mycosporine-glutamicol-glucoside have been reported in rock-inhabiting microcolonial fungi [51] and the terrestrial cyanobacteria from rock surfaces [52]. Hence, these glycosylated MAAs may have protective functions in general, allowing adaptation to terrestrial environments where they are exposed to drastic changes in temperature and extreme desiccation, as well as direct solar radiation in the biologically harmful UV range.

UV radiation causes oxidative damage in cyanobacterial cells, including lipid

peroxide formation, DNA strand breaks, and chlorophyll bleaching concomitant with deactivation of photosynthesis and growth inhibition [53]. MAAs are suggested to have a protective role against UV induced oxidative stress in algae [54] and cyanobacteria [55]. It has been reported that mycosporine-glycine shows radical scavenging activity *in vitro* [56-58]. These previous reports are in agreement with our results showing the radical scavenging activity found in the MAAs from *N. commune* (Table 6, Fig. 4), supporting the idea of multifunction MAAs [28, 29, 31]. The energy absorbed by MAAs is dispersed as heat [35, 36]; thus, it will be interesting to determine whether UV radiation affects the radical scavenging activity of the glycosylated MAAs in *N. commune*. *In vitro* studies will answer this question and provide further evidence of multifunctional compounds.

It has been reported that porphyra-334 has a photoprotective role but does not function as an antioxidant [35, 36, 56]. The 478-Da MAA in *N. commune* was characterized as a glycosylated porphyra-334 derivative (Fig. 2) and showed radical scavenging activity *in vitro* (Table 6). It will be interesting to determine whether the glycosylation of porphyra-334 found in *N. commune* is a unique adaptation in this organism for terrestrial environments. Biochemical and molecular biological studies of the biosynthesis of the 478-Da MAA in *N. commune* will give further insight into the diversity and function of MAAs.

It has been suggested MAAs may function as osmotic solutes because of the high concentrations of MAAs in halophilic cyanobacteria [59]. The amounts of MAAs detected in field-isolated natural colonies of *N. commune* were approximately 0.04% of their dry weight [60], in agreement with previous reports of the amounts of MAAs in cyanobacteria ranging from 0.06 to 0.8% [33, 61]. *N. commune* colonies contain a large amount of EPS, which accounts for up to 80% of their dry weight [12]; thus, the concentrations of MAAs per cell should not be underestimated. Trehalose is known to be a multifunctional molecule and dry colonies of *N. commune* accumulate trehalose levels ranging from 0.1 to 0.2% [19]. It has

been noted that the trehalose level in *N. commune* is too low to explain the extreme environmental stress tolerance of this organism; organisms with a trehalose producing capacity as high as 10 to 20% of their dry weight are known [62]. However, the trehalose concentration per cell may be underestimated in *N. commune* because of the presence of EPS. The unique glycosylated MAAs found in the cyanobacterium *N. commune* (Fig. 2, 3) imply that the MAA function together with EPS and trehalose can protect cells from damage during desiccation. Further studies on the novel MAAs in *N. commune* will be needed to address their functions in the mechanisms of anhydrobiosis.

Acknowledgments

We thank Dr. T. Tanaka for helpful suggestions, Dr. Y. Ukaji for generous assistance with IR analysis, Drs. T. Nishiuchi and T. Asano for MS analysis, Drs. T. Yamagaki and K. Sugase for NMR analysis, and Ms. A. Kondoh for technical assistance. This work was supported by Japan Society for the Promotion of Science (KAKENHI 22510227), Suntory Institute for Bioorganic Research (SUNBOR Grant) and HABA laboratories Inc. (a research grant).

Supporting Information

Figure S1 MALDI-TOF MS analysis of the purified MAAs. (A) MAA with absorption maximum at 335 nm. The molecular ion fragment at m/z 479 corresponds to [MAA+H^+]. (B) MAA with absorption maxima at 312 and 340 nm. The molecular ion fragment at m/z 1051 corresponds to [MAA+H^+].

Figure S2 FTIR spectra of the 478-Da MAA with absorption maximum at 335 nm (A) and the 1050-Da MAA with absorption maxima at 312 and 340 nm (B).

Figure S3 MS/MS analysis of the 478-Da MAA with absorption maximum at 335 nm. The

molecular ion fragment at m/z 479 shown in Fig. S1(A) was ionized and the secondary mass spectrum was recoded. The molecular ion fragment at m/z 347 corresponds to porphyra-334 with a molecular mass of 346.

Figure S4 LC-MS analysis of the thermal decomposed products of purified MAA with absorption maxima at 312 and 340 nm. (A) Changes of UV-VIS spectra during heat treatment at 100˚C. The fragments with absorption maxima at 312 nm and 335 nm (B), at 312 nm (C) and at 335 nm (D) were detected, respectively. The fragment with absorption maximum at 312 nm corresponds to a 3-aminocyclohexen-1-one derivative (C) and that with absorption maximum at 335 nm corresponds to a 1,3-diaminocyclohexen derivative (D).

Table S1 Summary of MS/MS analysis of the purified 1050-Da MAA with absorption maxima at 312 and 340 nm.

Table S2 Prediction of the thermal decomposition of the 1050-Da MAA with absorption maxima at 312 and 340 nm.

References

[1] D. Billi, M. Potts, Life and death of dried prokaryotes. Research in Microbiol. 153 (2002) 7-12.

[2] J.S. Clegg, Cryptobiosis - a peculiar state of biological organization. Comp. Biochem. Physiol. B Biochem. Mol. Biol. 128 (2001) 613-624.

[3] J.H. Crowe, J.F. Carpenter, L.M. Crowe, The role of vitrification in anhydrobiosis. Annu. Rev. Physiol. 60 (1998) 73-103.

[4] L.M. Crowe, Lessons from nature: the role of sugars in anhydrobiosis. Comp. Biochem. Physiol. A. Mol. Integr. Physiol. 131 (2002) 505-513.

[5] M. Potts, Desiccation tolerance: a simple process? Trends Microbiol. 9 (2001) 553-559.

[6] R.E. Cameron, Species of *Nostoc* vaucher occurring in the Sonoran Desert in Arizona. Trans. Amer. Microsc. Soc. 81 (1962) 379-384.

[7] C.B. Lipman, The successful revival of *Nostoc commune* from a herbarium specimen

eighty-seven years old. Bull. Torr. Bot. Club 68 (1941) 664-666.
[8] M. Potts, Desiccation tolerance of prokaryotes. Microbiol. Rev. 58 (1994) 755-805.
[9] M. Potts, Mechanisms of desiccation tolerance in cyanobacteria. Eur. J. Phycol. 34 (1999) 319-328.
[10] M. Potts, *Nostoc*, in: B.A. Whitton M. Potts (Eds.), The Ecology of Cyanobacteria, Kluwer Academic Publishers, Netherlands, 2000, pp. 465-504.
[11] D.J. Wright, S.C. Smith, V. Joardar, S. Scherer, J. Jervis, A. Warren, R.F. Helm, M. Potts, UV irradiation and desiccation modulate the three-dimensional extracellular matrix of *Nostoc commune* (cyanobacteria). J. Biol. Chem. 280 (2005) 40271-40281.
[12] F.M. Morsy, S. Kuzuha, Y. Takani, T. Sakamoto, Novel thermostable glycosidases in the extracellular matrix of the terrestrial cyanobacterium *Nostoc commune*. J. Gen. Appl. Microbiol. 54 (2008) 243-252.
[13] C. Bertocchi, L. Navarini, A. Cesàro, M. Anastasio, Polysaccharides from cyanobacteria. Carbohydrate Polymers. 12 (1990) 127-153.
[14] V. Gloaguen, H. Morvan, L. Hoffmann, Released capsular polysaccharides of Oscillatoriaceae (Cyanophyceae, Cyanobacteria). Algological Studies 78 (1995) 53-69.
[15] R.F. Helm, Z. Huang, D. Edwards, H. Leeson, W. Peery, M. Potts, Structural characterization of the released polysaccharide of desiccation-tolerant *Nostoc commune* DRH-1. J. Bacteriol. 182 (2000) 974-982.
[16] D.R. Hill, A. Peat, M. Potts, Biochemistry and structure of the glycan secreted by desiccation-tolerant *Nostoc commune* (cyanobacteria). Protoplasma 182 (1994) 126-148.
[17] D.R. Hill, T.W. Keenan, R.F. Helm, M. Potts, L.M. Crowe, J.H. Crowe, Extracellular polysaccharide of *Nostoc commune* (cyanobacteria) inhibits fusion of membrane vesicles during desiccation. J. Appl. Phycol. 9 (1997) 237-248.
[18] Y. Tamaru, Y. Takani, T. Yoshida, T. Sakamoto, Crucial role of extracellular polysaccharides in desiccation and freezing tolerance in the terrestrial cyanobacterium *Nostoc commune*. Appl. Environ. Microbiol. 71 (2005) 7327-7333.
[19] T. Sakamoto, T. Yoshida, H. Arima, Y. Hatanaka, Y. Takani, Y. Tamaru, Accumulation of trehalose in response to desiccation and salt stress in the terrestrial cyanobacterium *Nostoc commune.* Phycological Res. 57 (2009) 66-73.
[20] T. Yoshida, T. Sakamoto, Water-stress induced trehalose accumulation and control of trehalase in the cyanobacterium *Nostoc punctiforme* IAM M-15. J. Gen. Appl. Microbiol. 55 (2009) 135-145.
[21] N. Hershkovitz, A. Oren, Y. Cohen, Accumulation of trehalose and sucrose in

cyanobacteria exposed to matric water stress. Appl. Environ. Microbiol. 57 (1991) 645-648.
[22] K. Satoh, M. Hirai, J. Nishio, T. Yamaji, Y. Kashino, H. Koike, Recovery of photosynthetic systems during rewetting is quite rapid in a terrestrial cyanobacterium, *Nostoc commune*. Plant Cell Physiol. 43 (2002) 170-176.
[23] S. Scherer, A. Ernst, T.-W. Chen, P. Böger, Rewetting of drought-resistant blue-green algae: Time course of water uptake and reappearance of respiration, photosynthesis, and nitrogen fixation. Oecologia 62 (1984) 418-423.
[24] S. Fukuda, R. Yamakawa, M. Hirai, Y. Kashino, H. Koike, K. Satoh, Mechanisms to avoid photoinhibition in a desiccation-tolerant cyanobacterium, *Nostoc commune*. Plant Cell Physiol. 49 (2008) 488-492.
[25] M, Hirai, R. Yamakawa, J. Nishio, T. Yamaji, Y. Kashino, H. Koike, K. Satoh, Deactivation of photosynthetic activities is triggered by loss of a small amount of water in a desiccation-tolerant cyanobacterium, *Nostoc commune*. Plant Cell Physiol. 45 (2004) 872-878.
[26] W.M. Bandaranayake, Mycosporines: are they nature's sunscreens? Natural Product Reports 1998 (1998) 159-171.
[27] C.S. Cockell, J. Knowland, Ultraviolet radiation screening compounds. Biol. Rev. 74 (1999) 311-345.
[28] A. Oren, N. Gunde-Cimerman, Mycosporines and mycosporine-like amino acids: UV protectants or multipurpose secondary metabolites? FEMS Microbiol. Lett. 269 (2007) 1-10.
[29] R.P. Rastogi, R.P. Sinha, Biotechnological and industrial significance of cyanobacterial secondary metabolites. Biotechnology Advances 27 (2009) 521-539.
[30] J.M. Shick, W.C. Dunlap, Mycosporine-like amino acids and related gadusols: Biosynthesis, accumulation, and UV-protective functions in aquatic organisms. Annu. Rev. Physiol. 64 (2002) 223-262.
[31] S.P. Singh, D.-P. Häder, R.P. Sinha, Cyanobacteria and ultraviolet radiation (UVR) stress: Mitigation strategies. Ageing Research Reviews 9 (2010) 79-90.
[32] E.P. Balskus, C.T. Walsh, The genetic and molecular basis for sunscreen biosynthesis in cyanobacteria. Science 329 (2010) 1653-1656.
[33] F. Garcia-Pichel, R.W. Castenholz, Occurrence of UV-absorbing, mycosporine-like compounds among cyanobacterial isolates and an estimate of their screening capacity. Appl. Environ. Microbiol. 59 (1993) 163-169.
[34] F. Garcia-Pichel, C.E. Wingard, R.W. Castenholz, Evidence regarding the UV sunscreen

role of a mycosporine-like compound in the cyanobacterium *Gloeocapsa* sp. Appl. Environ. Microbiol. 59 (1993) 170–176.

[35] F.R. Conde, M.S. Churio, C.M. Previtali, The photoprotector mechanism of mycosporine-like amino acids. Excited-state properties and photostability of porphyra-334 in aqueous solution. J. Photochem. Photobiol. B. 56 (2000) 139-144.

[36] F.R. Conde, M.S. Churio, C.M. Previtali, The deactivation pathways of the excited-states of the mycosporine-like amino acids shinorine and porphyra-334 in aqueous solution. Photochem. Photobiol. Sci. 3 (2004) 960-967.

[37] G.A. Böhm, W. Pfleiderer, P. Böger, S. Scherer, Structure of a novel oligosaccharide-mycosporine-amino acid ultraviolet A/B sunscreen pigment from the terrestrial cyanobacterium *Nostoc commune*. J. Biol. Chem. 270 (1995) 8536-8539.

[38] P.J. Proteau, W.H. Gerwick, F. Garcia-Pichel, R. Castenholz, The structure of scytonemin, an ultraviolet sunscreen pigment from the sheaths of cyanobacteria. Experientia 49 (1993) 825-829.

[39] R.W. Castenholz, F. Garcia-Pichel, Cyanobacterial responses to UV-radiation, in: B.A. Whitton, M. Potts (Eds.), The Ecology of Cyanobacteria, Kluwer Academic Publishers, Netherlands, 2000, pp. 591-611.

[40] B. Shirkey, D.P. Kovarcik, D.J. Wright, G. Wilmoth, T.F. Prickett, R.F. Helm, E.M. Gregory, M. Potts Active Fe-containing superoxide dismutase and abundant *sodF* mRNA in *Nostoc commune* (cyanobacteria) after years of desiccation. J. Bacteriol. 182 (2000) 189-197.

[41] R. Re, N. Pellegrini, A. Proteggente, A. Pannala, M. Yang, C. Rice-Evans, Antioxidant activity applying an improved ABTS radical cation decolorization assay. Free Radical Biol. Medicine 26 (1999) 1231-1237.

[42] S. Takano, D. Uemura, Y. Hirata, Isolation and structure of a new amino acid, palythine, from the zoanthid *Palythoa tuberculosa*. Tetrahedron Letters 26 (1978) 2299-2300.

[43] A. Torres, C.D. Enk, M. Hochberg, M. Srebnik, Porphyra-334, a potential natural source for UVA protective sunscreens. Photochem. Photobiol. Sci. 5 (2006) 432-435.

[44] M. Yoshiki, K. Tsuge, Y. Tsuruta, T. Yoshimura, K. Koganemaru, T. Sumi, T. Matsui, K. Matsumoto, Production of new antioxidant compound from mycosporine-like amino acid, porphyra-334 by heat treatment. Food Chem. 113 (2009) 1127-1132.

[45] K. Whitehead, J.I. Hedges, Electrospray ionization tandem mass spectrometric and electron impact mass spectrometric characterization of mycosporine-like amino acids. Rapid Commun. Mass Spectrom. 17 (2003) 2133-2138.

[46] V. Roginsky, E.A. Lissi, Review of methods to determine chain-breaking antioxidant activity in food. Food Chem. 92 (2005) 235-254.

[47] M. Ehling-Schulz, W. Bilger, S. Scherer, UV-B-induced synthesis of photoprotective pigments and extracellular polysaccharides in the terrestrial cyanobacterium *Nostoc commune*. J. Bacteriol. 179 (1997) 1940-1945.

[48] D.R. Hill, S.L. Hladun, S. Scherer, M. Potts, Water stress proteins of *Nostoc commune* (cyanobacteria) are secreted with UV-A/B-absorbing pigments and associate with 1,4-β-D-xylanxylanohydrolase activity. J. Biol. Chem. 269 (1994) 7726-7734.

[49] S. Scherer, T.W. Chen, and P. Böger, A new UV-A/B protecting pigment in the terrestrial cyanobacterium *Nostoc commune*. Plant Physiol. 88 (1988) 1055-1057.

[50] S. Scherer, M. Potts, Novel water stress protein from a desiccation-tolerant cyanobacterium: purification and partial characterization. J. Biol. Chem. 264 (1989) 12546-12553.

[51] M. Volkmann, K. Whitehead, H. Rütters, J. Rullkötter, A.A. Gorbushina, Mycosporine-glutamicol-glucoside: a natural UV-absorbing secondary metabolite of rock-inhabiting microcolonial fungi. Rapid Commun. Mass Spectrom. 17 (2003) 897-902.

[52] M. Volkmann, A.A. Gorbushina, A broadly applicable method for extraction and characterization of mycosporines and mycosporine-like amino acids of terrestrial, marine and freshwater origin. FEMS Microbiol. Lett. 255 (2006) 286-295.

[53] Y.-Y. He, M. Klisch, D.-P. Häder, Adaptation of cyanobacteria to UV-B stress correlated with oxidative stress and oxidative damage. Photochem. Photobiol. 76 (2002) 188-196.

[54] T.-M. Lee, C.-T. Shiu, Implications of mycosporine-like amino acid and antioxidant defenses in UV-B radiation tolerance for the algae species *Ptercladiella capillacea* and *Gelidium amansii*. Marine Environmental Research 67 (2009) 8-16.

[55] L. Zhang, L. Li, Q. Wu, Protective effects of mycosporine-like amino acids of *Synechocystis* sp. PCC 6803 and their partial characterization. J. Photochem. Photobiol. B:Biology 86 (2007) 240-245.

[56] W.C. Dunlap, Y. Yamamoto, Small-molecule antioxidants in marine organisms: antioxidant activity of mycosporine-glycine. Comp. Biochem. Physiol. 112B (1995) 105-114.

[57] H.-J. Suh, H.-W. Lee, J. Jung, Mycosporine glycine protects biological systems against photodynamic damage by quenching single oxygen with a high efficiency. Photochem. Photobiol. 78 (2003) 109-113.

[58] I. Yakovleva, R. Bhagooli, A. Takemura, M. Hidaka, Differential susceptibility to

oxidative stress of two scleractinian corals: antioxidant functioning of mycosporine-glycine. Comp. Biochem. Physiol. B. 139 (2004) 721-730.
[59] A. Oren, Mycosporine-like amino acids as osmotic solutes in a community of halophilic cyanobacteria. Geomicrobiology J. 14 (1997) 231-240.
[60] T. Sakamoto, K. Kumihashi, S. Kunita, T. Masaura, K. Inoue-Sakamoto, M. Yamaguchi, The extracellular-matrix retaining cyanobacterium *Nostoc verrucosum* accumulates trehalose but is sensitive to desiccation. FEMS Microbiol. Ecol. (2011) in press.
[61] B. Büdel, U. Karsten, F. Garcia-Pichel, Ultraviolet-absorbing scytonemin and mycosporine-like amino acid derivatives in exposed, rock-inhabiting cyanobacterial linchens. Oecologia 112 (1997) 165-172.
[62] A.D. Elbein, Y.T. Pan, I. Pastuszak, D. Carroll, New insights on trehalose: a multifunctional molecule. Glycobiology 13 (2003) 17R-27R.
[63] P.K. Agrawal, NMR spectroscopy in the structural elucidation of oligosaccharides and glycosides. Phytochemistry 31 (1992) 3307-3330.
[64] C. Roullier, M. Chollet-Krugler, E.-M. Pferschy-Wenzig, A. Maillard, G.N. Rechberger, B. Legouin-Gargadennec, R. Bauer, J. Boustie, Characterization and identification of mycosporines-like compounds in cyanolichens. Isolation of mycosporine hydroxyglutamicol from *Nephroma laevigatum* Ach. Photochemistry 72 (2011) 1348-1357.

Legends to figures:

Fig. 1. UV spectra of the purified MAA in H_2O. (**A**) 478-Da MAA with absorption maximum at 335 nm (ε =33173 M^{-1} cm^{-1} at 335 nm). (**B**) 1050-Da MAA with absorption maxima at 312 nm (ε =58800 M^{-1} cm^{-1} at 312 nm).

Fig. 2. A predicted structure for 478-Da MAA with absorption maximum at 335 nm. Pentose is bound to porphyra-334.

Fig. 3. Components and predicted structure of 1050-Da MAA with absorption maxima at 312 and 340 nm. (A) 3-aminocyclohexen-1-one structure related to absorption maximum at 312 nm. (**B**) 1,3-diaminocyclohexen structure related to absorption maximum at 335 nm. (**C**) Pentose. (**D**) Hexose. (**E**) A predicted structure for 1050-Da MAA.

Fig. 4. Elution profile of water extract of *Nostoc commune* with the 1050-Da MAA fractionated with a reverse phase HPLC. (**A**) MAA was detected with A_{330}. (**B**) Radical scavenging activity was measured by the ABTS decolorization assay. The 1050-Da MAA was eluted together with its associated radical scavenging activity in the fractions of 60 and 62 min. The data from a single experiment are shown, but similar experiments were repeated independently at least three times, and the co-elution of MAA and radical scavenging activity was observed in all cases.

Fig. 5. Elution profile of water extract of *Nostoc commune* with the 478-Da MAA fractionated with a reverse phase HPLC. (**A**) MAA was detected with A_{330}. The 478-Da MAA was eluted in the fractions of 22 and 24 min. (**B**) Radical scavenging activity was measured by the ABTS decolorization assay. A main peak of radical scavenging activity was detected in the the fractions of 46 to 50 min. The data from a single experiment are shown, but similar experiments were repeated independently at least twice, and identical results were obtained in all cases.

1
2
3

Table 1
Purification of 478-Da MAA with absorption maximum at 335 nm from *Nostoc commune* [a].

Step	Volume (ml)	MAA concentration[b] (mg l^{-1})	MAA amount (mg)	Yield (%)
30% methanol extract	1460	11	16.4	100
100% methanol solution	400	28	11.3	69
30% methanol solution	150	108	16.2	99
100% methanol solution	50	210	10.5	64
0.2% acetic acid solution	8.5	932	7.9	48
Reverse phase HPLC	1.5	3667	5.5	34
Gel filtration	0.5	10000	5.0	31

[a] Dry colonies of *N. commune* (32 g) containing the MAA with absorption maximum at 335 nm were used as starting materials, and the MAA was purified as described in Materials and Methods.
[b] MAA concentration was determined using an absorption coefficient of 120 L g^{-1} cm^{-1} [33].

1
2
3

Table 2
Purification of 1050-Da MAA with absorption maxima at 312 and 340 nm from *Nostoc commune* [a].

Step	Volume (ml)	MAA concentration[b] (mg l^{-1})	MAA amount (mg)	Yield (%)
Water extract	172	11	1.83	100
70% ethanol solution	550	2	1.34	73
Vacuum concentration	6	220	1.32	72
Reverse phase HPLC	0.5	1760	0.88	45
Gel filtration	0.5	1550	0.75	38

[a] Dry colonies of *N. commune* (5 g) containing the MAA with absorption maxima at 312 and 340 nm were used as starting materials, and the MAA was purified as described in Materials and Methods.
[b] MAA concentration was determined using an absorption coefficient of 120 L g^{-1} cm^{-1} [33].

1
2
3

Table 3
Comparison of IR spectra of MAA.

478-Da MAA with A_{max} at 335 nm	Porphyra-334	1050-Da MAA with A_{max} at 312 and 340 nm	Palythine
		Wavenumber (cm^{-1})	
3400		3399	
	3300		3260
		2929	
1606	1600	1617	1609
1558	1540	1541	1540
1382	1380	1400	1378
1310			1305
1273		1275	1273
1132			1126
1072	1080	1076, 1046	1052
1006			

IR spectra were recorded with a Fourier transform infrared (FTIR) spectrometer (Jasco FT/IR-230) by the KBr disk method. The wavenumbers of absorption bands for the purified MAA are compared with those for known MAA porphyra-334 [43] and palythine [42]. The data for IR spectra are shown in the supplementary data (Fig. S3).

1
2
3

Table 4
Summary of NMR analysis of 478-Da MAA with absorption maximum at 335 nm.

	478-Da MAA with A_{max} at 335 nm		Porphyra-334		β-D-Xylose	
C#	^{13}C	^{1}H	^{13}C	^{1}H	^{13}C	^{1}H
1	161.6	-	161.6	-		
2	128.4	-	126.0	-		
3	163.2	-	163.2	-		
4	36.4	3.00	32.5	2.75		
5	73.1	-	71.3	-		
6	35.9	2.83	33.0	2.77		
7	77.7	3.90,3.67	67.1	3.61s		
8	62.2	3.70s	59.0	3.73s		
9	49.5	4.06d(2.4)	47.0	4.07s		
10	177.7	-	177.6	-		
11	67.3	4.09d(4.5)	64.0	4.12d(5.0)		
12	178.2	-	178.0	-		
13	71.0	4.31dq(6.5,4.5)	68.0	4.33m(5.0,6,4)		
14	22.3	1.26d(6.5)	19.0	1.26d(6.4)		
15	106.4	4.37d(7.6)			97.5	4.21
16	73.5	3.60dd(7.6,9.6)			75.1	3.14
17	75.0	3.68dd(9.6,3.6)			76.8	3.33
18	71.1	3.95m			70.2	3.51
19	69.1	3.92,3.65			66.1	3.88,3.21

NMR spectra were recorded with a Bruker Avance 750 or a Joel ECA600 spectrometer in D_2O as solvent. Chemical shifts (ppm) for the purified 478-Da MAA with A_{max} at 335 nm are compared with those for the known MAA porphyra-334 [43] and xylose [63]. Coupling constants (Hz) are shown in parentheses. The data for NMR spectra are shown in the supplementary data.

Table 5
Summary of NMR analysis of 1050-Da MAA with absorption maxima at 312 and 340 nm.

Porphyra-334			Mycosporine hydroxyglutamicol			1050-Da MAA with A_{max} at 312 and 340 nm	
C#	^{13}C	^{1}H	C#	^{13}C	^{1}H	^{13}C	^{1}H
1	161.6	-				162.3	-
2	126.0	-				128.4	-
3	163.2	-				162.0	-
4	32.5	2.75				35.7	2.85d(17.2), 2.79d(16.8)
6	33.0	2.77				36.3	2.78d(16.2), 2.76d(15.1)
8	59.0	3.73s				62.2	3.65s
			1	185.9	-	187.2,187.2	-
			2	131.0	-	132.9	-
			3	159.9	-	162.5	-
			4	33.9	2.89m,2.89m	36.3	3.06d(17.5), 3.02d(17.2), 2.85d(17.2), 2.81d(17.5)
			6	43.2	2.44d(16.9), 2.69d(16.9)	45.6,45.6	2.65d(16.8), 2.65d(16.8), 2.65d(17.1), 2.66d(16.8)
			8	60.0	3.59s	62.3	3.54s, 3.54s

β-D-Glucose C-1		1050-Da MAA with A_{max} at 312 and 340 nm	
^{13}C	^{1}H	^{13}C	^{1}H
96.8	4.64	107.6	4.62d(7.9)
		105.0	4.5d(7.6)

NMR spectra were recorded with a Joel ECA600 spectrometer in D_2O as solvent. Chemical shifts (ppm) for the purified 1050-Da MAA with A_{max} at 312 and 340 nm are compared with those for the known MAA porphyra-334 [43] mycosporine hydroxyglutamicol [64] and glucose [63]. Coupling constants (Hz) are shown in parentheses. The data for NMR spectra

are shown as a supplement.

Table 6
Radical scavenging activity in MAA[a].

Assay	Colorimetry[b]	ESR[c]	
Substrate	ABTS	ABTS	DPPH
		IC_{50}(μM)	
Trolox[d]	272	182	128
478-Da MAA with A_{max} at 335 nm	9507	185	-
1050-Da MAA with A_{max} at 312 and 340 nm	1045	55	809

[a] Radical scavenging activity was measured using ABTS or DPPH as organic radical sources.
[b] Decolorization of ABTS was monitored with a spectrophotometer for 1 h.
[c] ESR signals were monitored with a free radical monitor (Joel JES-FR30EX).
[d]Trolox was used for a standard.
-, not detected.
IC_{50} (50% inhibitory concentration) are shown

Novel MAA from *Nostoc commune*

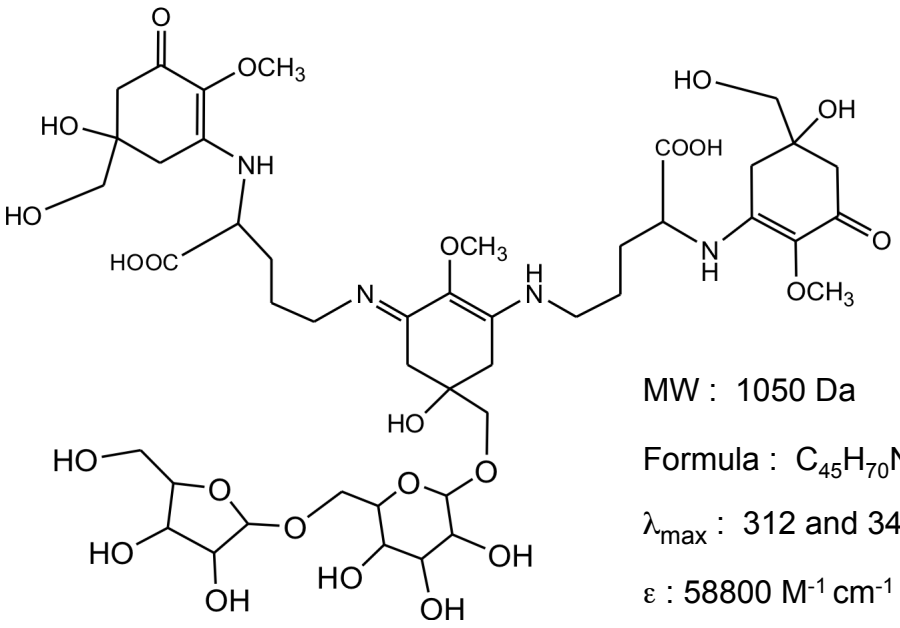

MW : 1050 Da

Formula : $C_{45}H_{70}N_4O_{24}$

λ_{max} : 312 and 340 nm

ε : 58800 $M^{-1}\,cm^{-1}$ at 312 nm

Fig. 1.

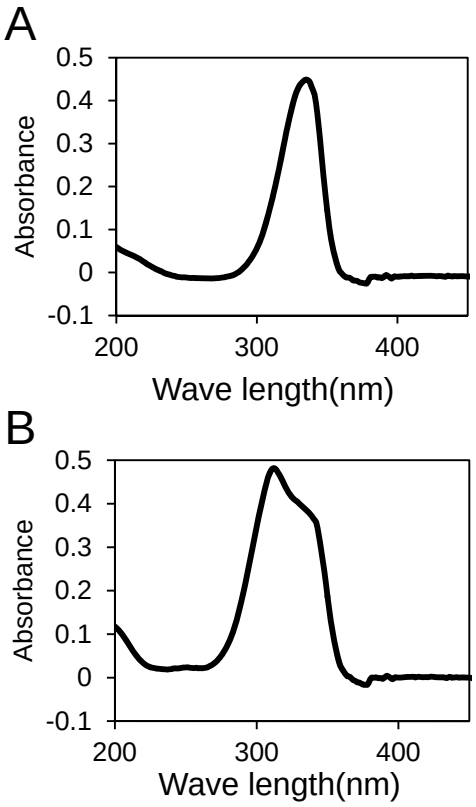

FIG. 1. UV spectra of the purified MAA in H_2O. (A) 478-Da MAA with absorption maximum at 335 nm (ε =33173 M^{-1} cm^{-1} at 335 nm). (B) 1050-Da MAA with absorption maxima at 312 nm (ε =58800 M^{-1} cm^{-1} at 312 nm).

Fig. 2.

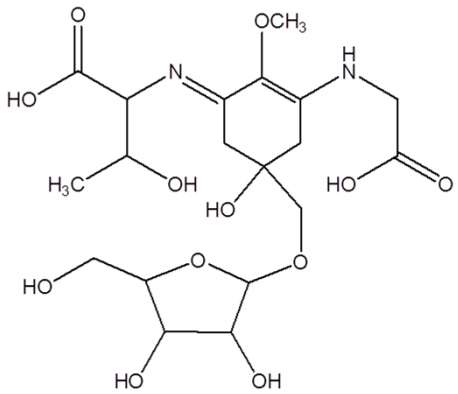

MW : 478

Formula : $C_{19}H_{30}N_2O_{12}$

FIG. 2. A predicted structure for 478-Da MAA with absorption maximum at 335 nm. Pentose is bound to porphyra-334.

Fig. 3.

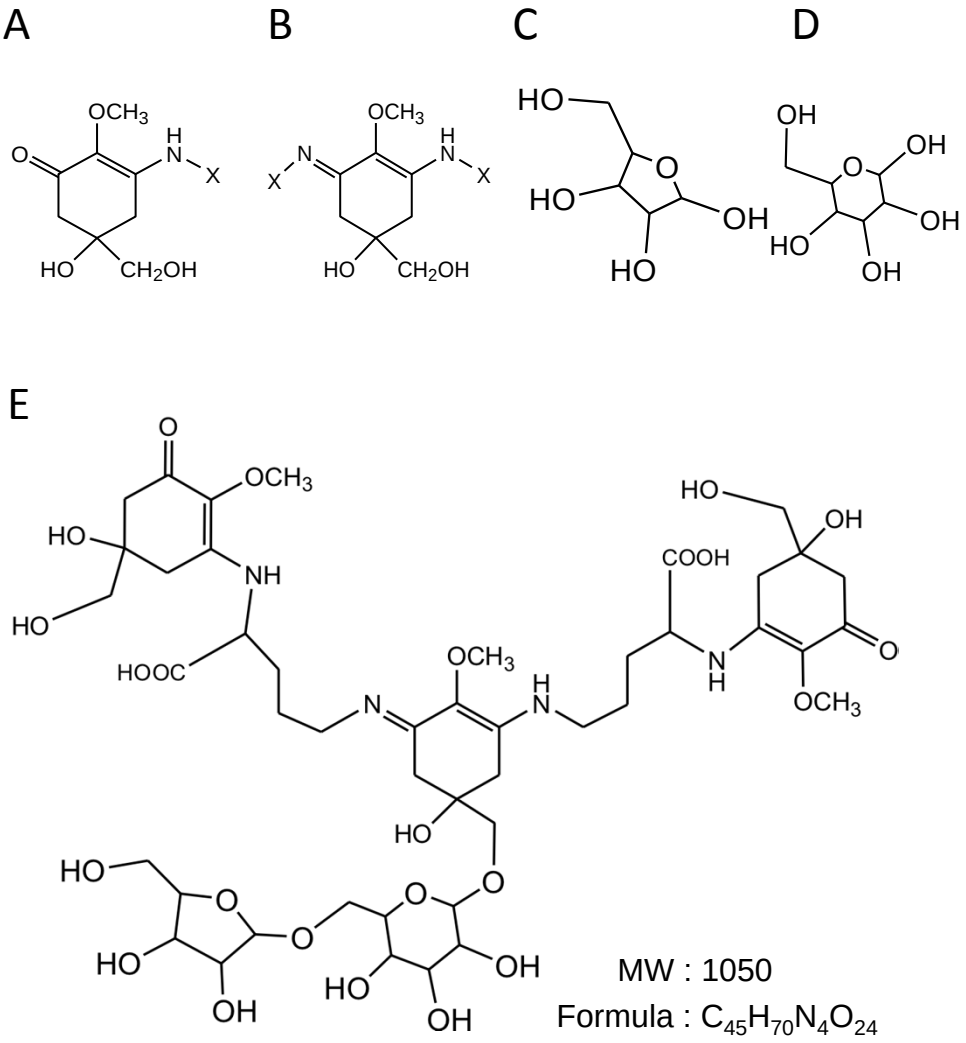

FIG. 3. Components and predicted structure of 1050-Da MAA with absorption maxima at 312 and 340 nm. (A) 3-aminocyclohexen-1-one structure related to absorption maximum at 312 nm. (B) 1,3-diaminocyclohexen structure related to absorption maximum at 335 nm. (C) Pentose. (D) Hexose. (E) A predicted structure for 1050-Da MAA.

Fig. 4.

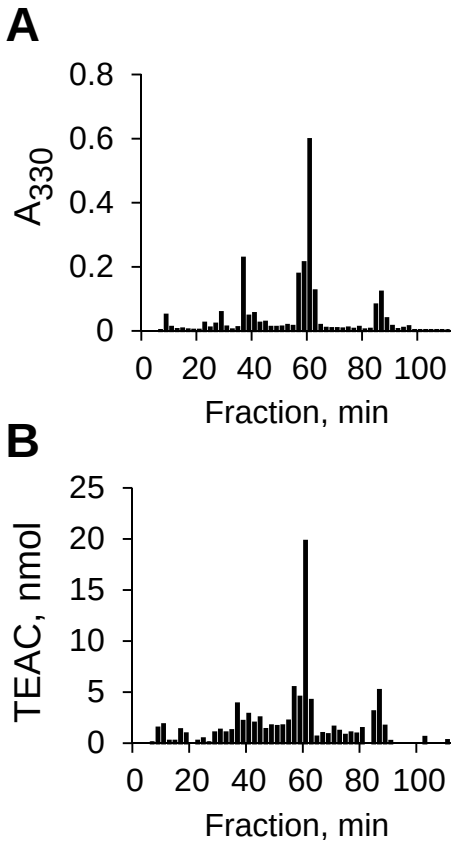

FIG. 4. Elution profile of water extract of *Nostoc commune* fractionated with a reverse phase HPLC. (A) MAA was detected with A_{330}. (B) Radical scavenging activity was measured by the ABTS decolorization assay. The 1050-Da MAA was eluted together with its associated radical scavenging activity in the fractions of 60 and 62 min. The data from a single experiment are shown, but similar experiments were repeated independently at least three times, and the co-elution of MAA and radical scavenging activity was observed in all cases.

Fig. S1.

A. MAA with Amax at 335 nm

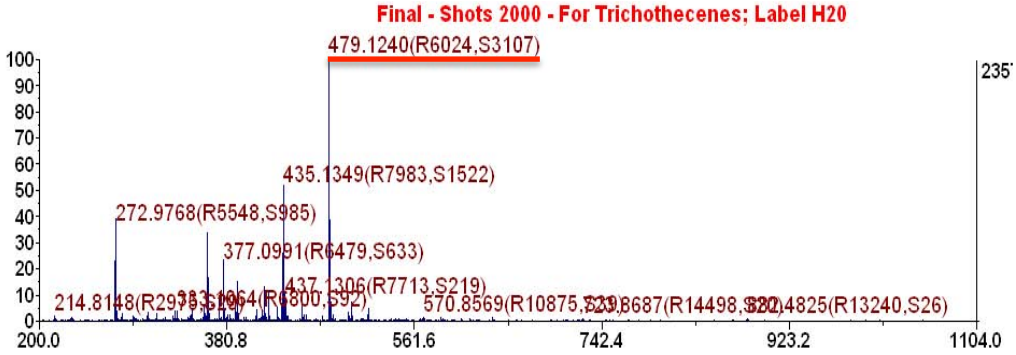

B. MAA with Amax at 312 and 340 nm

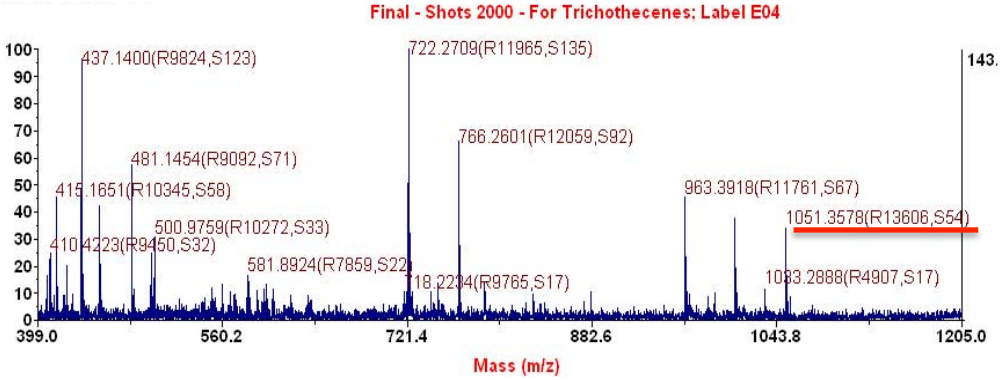

Fig. S1. MALDI-TOF MS analysis of the purified MAAs. (A) MAA with absorption maximum at 335 nm. The molecular ion fragment at m/z 479 corresponds to [MAA+H^+]. (B) MAA with absorption maxima at 312 and 340 nm. The molecular ion fragment at m/z 1051 corresponds to [MAA+H^+].

Fig. S2.

A. MAA with A_{max} at 335 nm

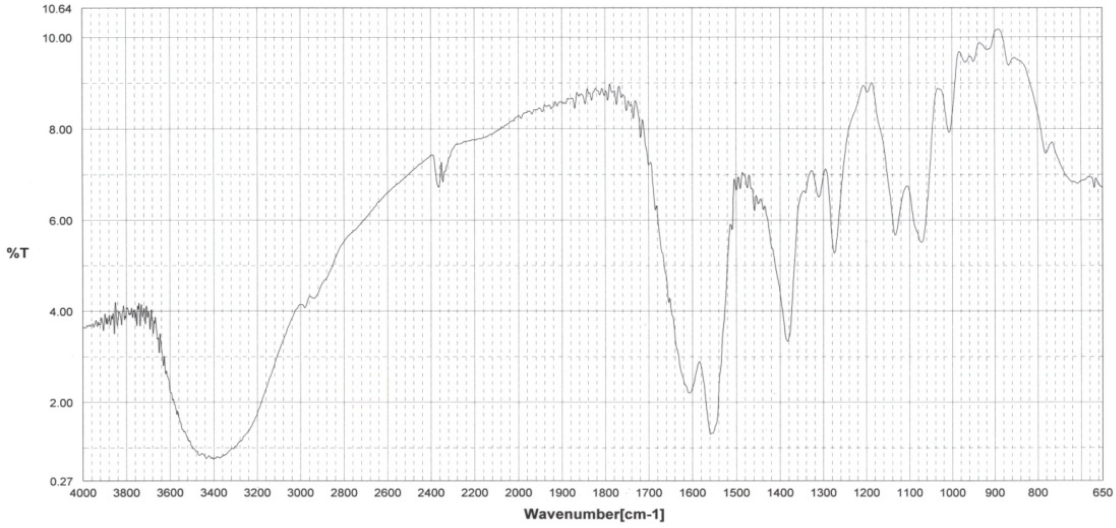

B. MAA with A_{max} at 312 and 340 nm

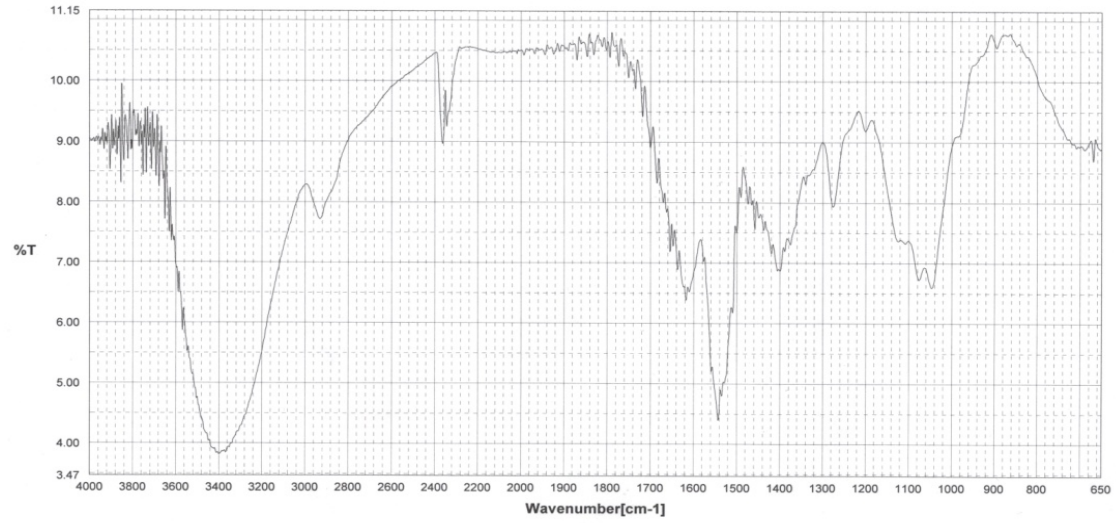

Fig. S2. FTIR spectra of the 478-Da MAA with absorption maximum at 335 nm (A) and the 1050-Da MAA with absorption maxima at 312 and 340 nm (B).

Fig. S3.

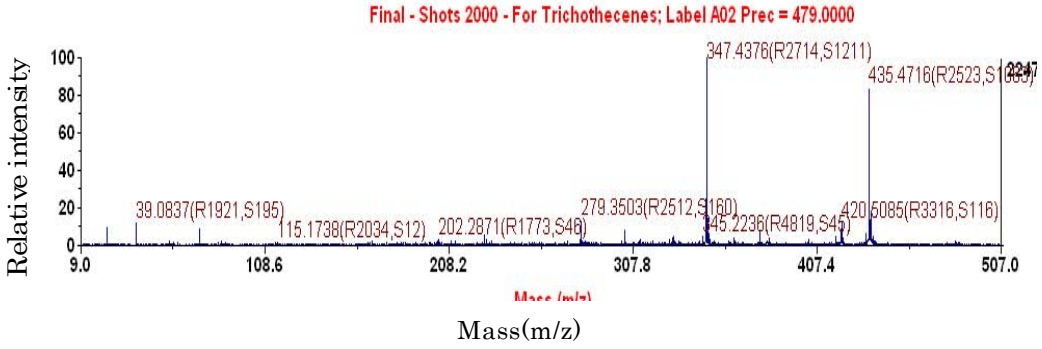

Mass of fragment [M+H$^+$]	Relative abundance	Neutral loss	Deleted fragment
479.12			
435.47	88	43.65	CO_2
420.51	10	58.62	CO_2+CH_3
347.44	100	131.69	Pentose ($C_5H_8O_4$)
279.35	13	199.77	

Fig. S3. MS/MS analysis of the 478-Da MAA with absorption maximum at 335 nm. The molecular ion fragment at m/z 479 shown in Fig. S1(A) was ionized and the secondary mass spectrum was recoded. The molecular ion fragment at m/z 347 corresponds to porphyra-334 with a molecular mass of 346.

Fig. S4.

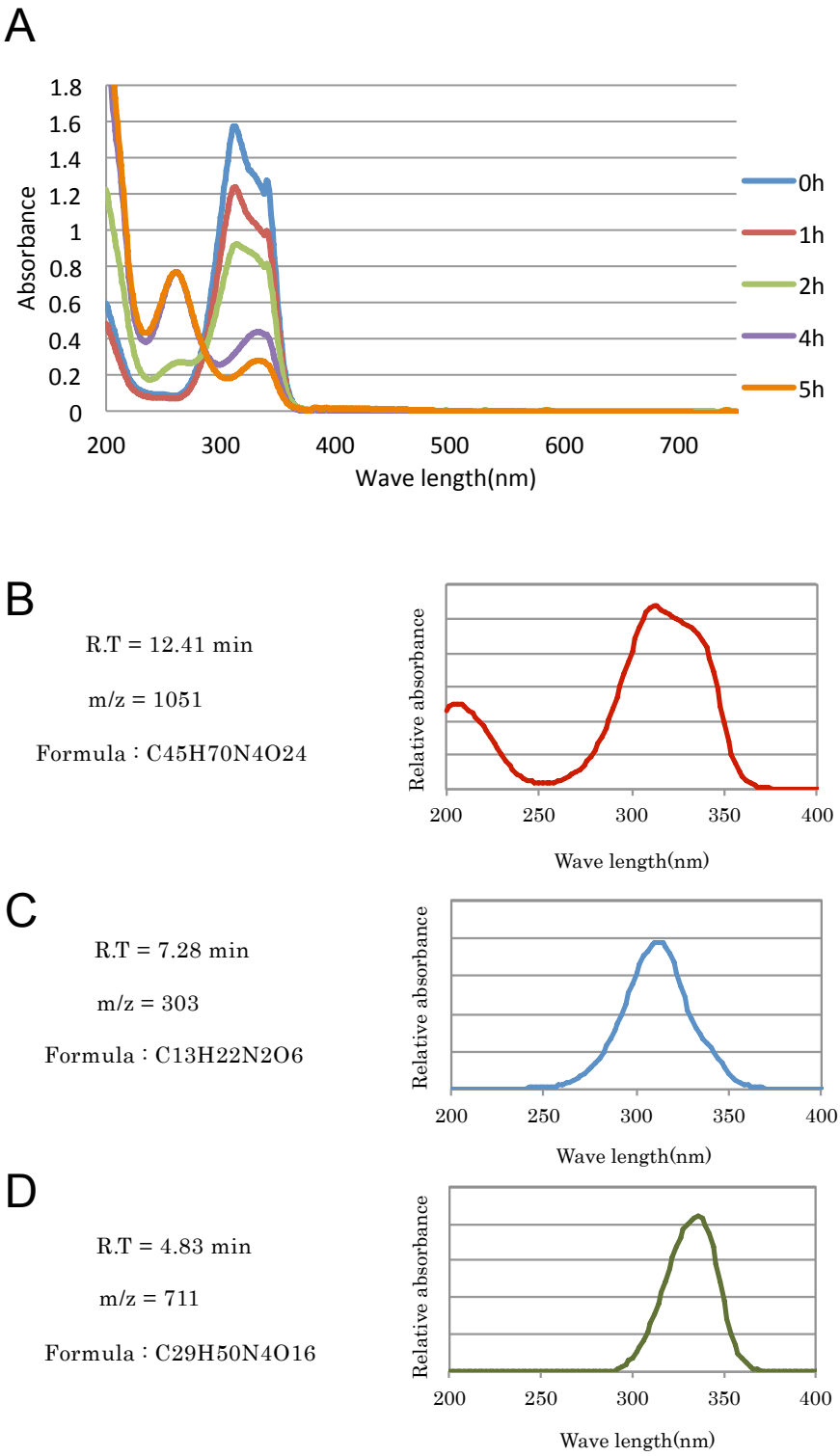

Fig. S4. LC-MS analysis of the thermal decomposed products of purified MAA with absorption maxima at 312 and 340 nm. (A) Changes of UV-VIS spectra during heat treatment at 100˚C. The fragments with absorption maxima at 312 nm and 335 nm (B), at 312 nm (C) and at 335 nm (D) were detected, respectively. The fragment with absorption maximum at 312 nm corresponds to a 3-aminocyclohexen-1-one derivative (C) and that with absorption maximum at 335 nm corresponds to a 1,3-diaminocyclohexen derivative (D).

Table S1. Summary of MS/MS analysis of the purified 1050-Da MAA with absorption maxima at 312 and 340 nm.

MS^2	Mass of fragment $[M+H^+]$	Relative abundance	Neutral loss	Deleted fragment
	1051.45			
	1033.20	98	18	H_2O
	1015.35	100	36	2 H_2O
	883.15	5	168	
	685.25	5	366	
	667.25	6	384	
	649.26	6	402	
MS^3	Mass of fragment $[M+H^+]$	Relative abundance	Neutral loss	Deleted fragment
	1015.35			
	997.37	47	18	
	883.33	100	132	Pentose
	667.18	26	348	
	649.17	90	366	
	603.37	29	412	
MS^4	Mass of fragment $[M+H^+]$	Relative abundance	Neutral loss	Deleted fragment
	883.33			
	865.41	60	18	H_2O
	721.15	6	162	Hexose
	667.30	20	216	3 H_2O+Hexose
	649.20	100	234	4 H_2O+Hexose
	603.25	30	280	
	349.26	38	534	
MS^5	Mass of fragment $[M+H^+]$	Relative abundance	Neutral loss	Deleted fragment
	649.20			
	613.60	26	36	2 H_2O
	603.39	100	46	Characteristic of MAA
	573.01	47	76	
	554.96	37	94	
	420.99	38	228	
	349.32	52	300	
	303.46	7	346	

Table S2. Prediction of the thermal decomposition of the 1050-Da MAA with absorption maxima at 312 and 340 nm.

A	Detected Mass [M+H$^+$]	Neutral loss	Expected formula	Deleted fragment
	1051.40		$C_{45}H_{70}N_4O_{24}$	
	1015.43	35.98	$C_{45}H_{66}N_4O_{22}$	2 H_2O
	883.38	168.02	$C_{40}H_{58}N_4O_{18}$	2 H_2O + Pentose ($C_5H_8O_4$)
	721.33	330.07	$C_{34}H_{48}N_4O_{13}$	2 H_2O + Pentose ($C_5H_8O_4$) + Hexose ($C_6H_{10}O_5$)
	419.18	632.22	$C_{21}H_{26}N_2O_7$	2 H_2O + Pentose ($C_5H_8O_4$) + Hexose ($C_6H_{10}O_5$) + $C_{13}H_{22}N_2O_6$
	303.16	748.25	$C_{13}H_{22}N_2O_6$	2 H_2O + Pentose ($C_5H_8O_4$)+ Hexose ($C_6H_{10}O_5$) + $C_{21}H_{26}N_2O_7$

B	Detected Mass [M+H$^+$]	Neutral loss	Expected formula	Deleted fragment
	1051.40		$C_{45}H_{70}N_4O_{24}$	
	881.39	170.01	$C_{37}H_{60}N_4O_{20}$	$C_8H_{10}O_4$
	711.33	341.08	$C_{29}H_{50}N_4O_{16}$	$C_8H_{10}O_4$ + $C_8H_{10}O_4$
	189.08	862.32	$C_8H_{12}O_5$	$C_{37}H_{58}N_4O_{19}$

C	Detected Mass [M+H$^+$]	Neutral loss	Expected formula	Deleted fragment
	1051.40		$C_{45}H_{70}N_4O_{24}$	
	718.30	333.10	$C_{31}H_{47}N_3O_{16}$	$C_{14}H_{23}N_1O_8$
	586.26	465.14	$C_{26}H_{39}N_3O_{12}$	$C_{14}H_{23}N_1O_8$ + Pentose ($C_5H_8O_4$)
	424.21	627.19	$C_{20}H_{29}N_3O_7$	$C_{14}H_{23}N_1O_8$ + Pentose ($C_5H_8O_4$) + Hexose ($C_6H_{10}O_5$)

The thermal decomposition products of the purified 1050-Da MAA with absorption maxima at 312 and 340 nm were analyzed by LC-MS.

A. The fragments detected in the MS analysis (Fig. S2B, Table S1) are shown.

B. The fragments deleted with a 170-Da unit of $C_8H_{10}O_4$.

C. The fragments deleted with pentose and hexose.